



Published in final edited form as:

J Cell Biochem. 2016 July ; 117(7): 1556–1567. doi:10.1002/jcb.25447.

Calcium sensing receptor function supports osteoblast survival and acts as a co-factor in PTH anabolic actions in bone

Saja A. Al-Dujaili¹, Amy J. Koh¹, Ming Dang², Xue Mi², Wenhan Chang³, Peter X. Ma^{2,4,5,6}, and Laurie K. McCauley^{1,7,*}

¹Department of Periodontics and Oral Medicine, University of Michigan

²Macromolecular Science and Engineering Center, University of Michigan

³Endocrine Research Unit, University of California – San Francisco

⁴Department of Biologic and Materials Sciences, University of Michigan

⁵Department of Materials Science and Engineering, University of Michigan

⁶Department of Biomedical Engineering, University of Michigan

⁷Department of Pathology, University of Michigan

Abstract

Anabolic actions of PTH in bone involve increased deposition of mineralizing matrix. Regulatory feedback of the process may be important to maintain calcium homeostasis and, in turn, calcium may inform the process. This investigation clarified the role of calcium availability and the calcium sensing receptor (CaSR) in the anabolic actions of PTH. CaSR function promoted osteoblastic cell numbers, with lower cell numbers in post-confluent cultures of primary calvarial cells from Col1-CaSR knock-out (KO) mice, and for calvarial cells from wild-type (WT) mice treated with a calcilytic. Increased apoptosis of calvarial cells with calcilytic treatment suggested CaSR is critical for protection against stage-dependent cell death. Whole and cortical, but not trabecular, bone parameters were significantly lower in Col1-CaSR KO mice versus WT littermates. Intact Col1-CaSR KO mice had lower serum P1NP levels relative to WT. PTH treatment displayed anabolic actions in WT and, to a lesser degree, KO mice, and rescued the lower P1NP levels in KO mice. Furthermore, PTH effects on whole tibiae were inhibited by osteoblast-specific CaSR ablation. Vertebral body implants (vossicles) from untreated Col1-CaSR KO and WT mice had similar bone volumes after 4 weeks of implantation in athymic mice. These findings suggest that trabecular bone formation can occur independently of the CaSR, and that the CaSR plays a collaborative role in the PTH anabolic effects on bone.

Keywords

parathyroid hormone; calcium sensing receptor; calcium; osteoblasts

*Address all correspondence to: Laurie K. McCauley, DDS, PhD, University of Michigan, School of Dentistry, 1011 N. University Ave, Ann Arbor, MI 48109-1078, Tel: +1-734-763-3311, mccauley@umich.edu.

Introduction

Calcium is a critical secondary messenger and regulator of biological functions. Osteoclasts liberate extracellular calcium [Ca^{2+}] from the matrix during bone resorption, producing a local calcium concentration of up to 40 mM [Silver et al., 1988]. Increased [Ca^{2+}] promotes osteoblast recruitment, proliferation and differentiation, and controls further osteoclast function [Miyachi et al., 1990; Zaidi et al., 1989]. While other factors have been suggested to couple bone resorption and formation (e.g. TGF- β) [Ota et al., 2013; Tang et al., 2009], the resorption-induced increase in [Ca^{2+}] levels has also been suggested to be a coupling mediator between osteoclasts and osteoblasts during normal bone remodeling and pathological states [Liao et al., 2006; Sugimoto et al., 1993]. Despite this vital role, the mechanisms for sensing and regulation of extracellular calcium levels lack clarity.

Serum calcium levels are tightly regulated and respond to changes in parathyroid hormone (PTH) secretion [Boden and Kaplan, 1990; Mundy and Guise, 1999]. PTH, with its key anabolic effects, is currently a therapy for osteoporosis, and is being investigated for use in localized craniofacial and long bone defects [Bashutski et al., 2010; Poole and Reeve, 2005]. While the mechanisms for the anabolic actions of PTH in bone are not entirely clear, it is postulated that PTH may support osteoprogenitor cell proliferation and early osteoblast survival, and regulate transcription and growth factors [Chen et al., 2002; Koh et al., 2011; Wu et al., 2010].

PTH is released by parathyroid cells in response to a decrease in [Ca^{2+}] levels to promote liberation of [Ca^{2+}] from the bone matrix through the process of bone resorption, and increased calcium reabsorption by the kidneys. Elevated [Ca^{2+}] levels suppress PTH production, acting as a feedback mechanism for PTH-regulated serum calcium homeostasis. The calcium sensing receptor (CaSR), a membrane-bound G protein-coupled receptor, plays a key role in maintaining calcium homeostasis by regulating parathyroid hormone (PTH) secretion and urinary calcium excretion [Brown, 2007; Goltzman and Hendy, 2015]. CaSR-deficiency in patients manifests as a rickets-like bone phenotype with mild to severe hyperparathyroidism, high serum calcium (hypercalcemia) and low urinary calcium (hypocalciuria) [Brown and MacLeod, 2001; Brown et al., 1998]. Similarly, transgenic mice with a CaSR deletion have an undermineralized skeleton at birth, hypercalcemia and increased morbidity [Garner et al., 2001; Ho et al., 1995]. The mineralization defect in CaSR-deficient mice is clearly maladaptive from a bone structural perspective, and may contribute to their hypercalcemia. Those phenotypes notwithstanding, impaired matrix mineralization may still have some adaptive value when serum calcium is low, and/or when osteoblasts lacking a functional CaSR are incapable of assessing ambient calcium concentrations. When calcium demand is increased, osteoid mineralization can be used to promote hypocalcemia and maintain normal overall serum calcium levels despite severe impairment of intestinal calcium absorption [Kostenuik et al., 2015; Lieben et al., 2012]. While not involving altered CaSR signaling capacity, this highlights the potential value of a regulatory mechanism by which osteoblasts can sense ambient calcium, and appropriately adjust osteoid production and/or its mineralization in a manner that mitigates the risk of hypocalcemia.

Deletion of the CaSR in osterix and collagen I (2.3 and 3.6 kb) expressing cells revealed the importance of the CaSR in the proliferation, survival and maturation of early osteoblasts [Chang et al., 2008; Riccardi et al., 2013]. Osteocalcin and Dmp-1 specific knock-outs of CaSR in mature osteoblasts were found to negatively regulate osteoclasts through the RANKL/OPG pathway [Chang et al., 2008; Riccardi et al., 2013]. However, skeletal defects in mice resulting from a global CaSR deletion were partially rescued by PTH deficiencies (e.g. crossing with PTH-null or parathyroid gland-deficient mice), suggesting that the CaSRs expressed outside of parathyroid glands are less critical for bone development [Ho et al., 1995; Kos et al., 2003; Tu et al., 2003].

Thus, while $[Ca^{2+}]$ is important in osteoblasts [Dvorak and Riccardi, 2004; Marie, 2010; Riccardi et al., 2013] and has been implicated indirectly in bone through PTH or other endocrine factors [Cheng et al., 2013], the role of the CaSR in bone remains controversial. In this study, the role of exogenous calcium administration and the CaSR on osteoblast proliferation and bone formation was determined both *in vitro* and *in vivo*. The findings demonstrate the calcium dose-dependency of osteoblasts, and suggest that the CaSR plays a contributing role in protecting osteoblasts against apoptosis. A possible role of the CaSR in the PTH anabolic effects in bone was also investigated, with resulting data suggesting interactions between PTH and calcium, through the CaSR, that may contribute to calcium homeostasis.

Materials and Methods

Calvarial cell isolation

Calvaria were harvested from 3 to 7 day old C57BL/6 mice (The Jackson Laboratories, Bar Harbor, ME) after euthanasia under an institutionally approved protocol. Digestion medium was prepared by adding 0.2% collagenase-A (Roche Applied Science, Indianapolis, IN), 10% trypsin and 1% penicillin-streptomycin-glutamine (PSG) to alpha-MEM (Invitrogen, Grand Island, NY). Cells were isolated by three serial incubations of calvaria in digestion medium at 37°C with gentle agitation. Supernatant from the first two incubations (15 and 20 minutes, respectively) were discarded, and fresh digestion medium was added each time. Supernatant from the last incubation (1 hour) was filtered through a 100 µm cell strainer. The eluted cells were then centrifuged, resuspended in growth medium (10% FBS, 1% PSG in alpha-MEM), and seeded in 24-well plates at a density of approximately 2×10^4 cells per well.

In vitro enumeration assays

Calvarial cells were cultured overnight in alpha-MEM medium containing 1.8 mM $CaCl_2$ (Invitrogen) to allow equal initial seeding and adhesion in all groups prior to treatment with different doses of calcium. Calcium chloride ($CaCl_2$; Sigma-Aldrich, St Louis, MO) was added to calcium-free DMEM (Invitrogen) containing 10% FBS, 1% PSG to achieve final concentrations of 0 to 5 mM. Cells were detached from their wells using 0.25% trypsin-EDTA (Invitrogen) at different time points (up to 14 days) to assess cell numbers using trypan blue exclusion. In other experiments, cells were treated with either calcimimetic, R-568 (1 µM, Tocris Bioscience, Bristol, UK), calcium sensing receptor antagonist, NPS

2143 (1 μ M, Santa Cruz Biotechnology, Dallas, TX), or vehicle (DMSO) for 14 days to assess the effects of the compounds on cell number using the trypan blue exclusion method. Cell death was quantified using ELISA for histone-complexed DNA fragments (Roche), per the manufacturer's protocol.

Animal breeding and care

The $Col\text{-}BoneCaSR^{flox/flox}$ mice with osteoblast-specific CaSR ablation were generated as previously described [Chang et al., 2008]. Briefly, floxed CaSR mice were bred with mice expressing the 2.3kb Col(I) Cre transgene. To identify genotypes, genomic DNA was extracted from mouse tails using a REDExtract-N-Amp Tissue PCR Kit (Sigma-Aldrich) and amplified by PCR with specific primers (Supplementary Table 1), with the final PCR products run in a 3% agarose gel (Supplementary Figure 3A). Homozygous knockout, $Col\text{-}BoneCaSR^{flox/flox}$ (KO) mice had stunted growth and severe skeletal development compared to control wild-type and heterozygous littermates (WT).

All animals were fed rodent chow containing 0.95% calcium and 0.7% phosphorus (LabDiet, St Louis, MO), and were housed and cared for by the Unit for Laboratory Animal Medicine. Procedures were approved by the University of Michigan Committee for the Use and Care of Animals and performed in accordance with institutional ethical requirements.

RT-PCR

Calvaria were isolated from 4–5 day old $Col\text{-}BoneCaSR^{flox/flox}$ (KO) mice and control littermates (WT), frozen in liquid nitrogen, and crushed using a mortar and pestle. Total RNA was extracted using TRIzol reagent (Invitrogen) and purified using RNeasy Mini Kit (Qiagen, Valencia, CA), per manufacturers' protocols. cDNA was reverse-transcribed from 0.6 μ g RNA in 1 μ l reaction mixture using the TaqMan RT-PCR system (Applied Biosystems, Branchburg, NJ). TaqMan Master Mix and primer/probe sets (Applied Biosystems) were used to amplify genes of interest: RUNX-2 (Mm00501584_m1), osterix/Sp7 (NM_130458), and osteocalcin/Bglap1 (Mm03413826_mH). GAPDH (Hs99999915_m1) was used as an endogenous control. PCR was performed using the ABI Prism 7700 Sequence Detection System (Applied Biosystems) in triplicate, and Ct values were calculated as an average of each triplicate per sample. Ct values of the genes of interest for each sample were normalized to the corresponding Ct value of GAPDH ($- Ct$).

Ectopic ossicle model

Bone marrow stromal cells (BMSCs) were isolated from femurs and tibiae of 4–8 week old C57BL/6 luciferase transgenic mice (B6; C3-Tg (TetTALuc) 1Dgs/J, Jackson Labs) as described previously [Pettway and McCauley, 2008; Pettway et al., 2008]. Expression of the luciferase transgene in individual mice was first confirmed using bioluminescent imaging (BLI, see below). Cells were isolated by flushing media (20% FBS, 1% PSG, 10 nM dexamethasone (Sigma) in alpha-MEM) through the marrow cavity of each bone. Bone marrow cells from two mice were pooled, plated onto a single T-75 flask, and cultured until confluence (approx. 1 week), at which point they were detached using 0.25% trypsin-EDTA and re-plated onto two T-75 flasks for another 3–5 days. Upon confluence, cells were trypsinized and seeded onto poly(L-lactic acid) scaffolds [He et al., 2010; Wei and Ma,

2006] containing different amounts of calcium phosphate (0–1.2 mg). Before cell seeding, scaffolds were primed and sterilized by incubating with 70% ethanol under vacuum (13 psi) for 30 minutes, washed twice with sterile PBS for 20 minutes each, and immersed in cell growth medium for 30 minutes. Excess media was gently aspirated before seeding cells at a density of $1\text{--}2.5 \times 10^6$ cells per scaffold. Cell seeded scaffolds (ossicles) were placed on ice until implantation into subcutaneous pockets in 4 week old male athymic mice (Harlan Laboratories, Haslett, MI), then left for four weeks until sacrifice and harvesting of ossicles for analyses.

Ectopic vossicle model

Ten days old male and female *Col-BoneCaSR^{flox/flox}* (KO) mice and control (WT) littermates, which carried homozygous floxed-CaSR alleles without Cre expression, were euthanized and the lumbar region of their spine was harvested for individual vertebral bodies (vossicles), as described previously [Koh et al., 2005; Pettway and McCauley, 2008]. Longitudinal skin incisions (1–2 cm long) were made on both the right and left sides of the dorsal surface of 4–6 week old male athymic mice (Harlan Laboratories), creating four subcutaneous pockets. Four vossicles from a single donor mouse were implanted subcutaneously into a single host athymic mouse to reduce variability. After four weeks of implantation, animals were sacrificed and vossicles harvested for analyses.

Bioluminescent imaging (BLI)

In vivo bioluminescence was measured using the IVIS 200 imaging system (PerkinElmer, Hopkinton, MA, USA) at the University of Michigan Cellular and Molecular Imaging Center. Mice were injected with 100 μ l of 40 mg/ml D-luciferin in PBS (approx. 20 mg/kg) intraperitoneally, and anesthetized using a 2% isoflurane/air mixture. Image acquisition was initiated approximately 12 minutes after injection of D-luciferin. Living Image 3.0 software was used for data analysis (PerkinElmer). Regions of interest corresponding to the implanted ossicles were defined to quantify the photon distribution.

***In vivo* PTH treatment regimen**

Four-day old CaSR pups were injected with either 50 μ g/kg/d human PTH (1–34) (Bachem, Torrance, CA) or vehicle (saline) subcutaneously for 17 days, as previously described [30]. Mouse weight was measured daily to determine the injection dose. Animals were sacrificed one day after the last injection (day 18), and blood and bones were collected. Bones were imaged using x-ray radiography after fixation.

Serum Analysis

At sacrifice, mice were anesthetized and whole blood collected from cardiac puncture. Serum was isolated from mouse whole blood by centrifugation at 8,000 rpm. P1NP was measured using a mouse serum ELISA (Immunodiagnostic Systems, Scottsdale, AZ), per the manufacturer's protocol.

microCT

Specimens were embedded in 1% agarose and placed in a 19 mm diameter tube and scanned over their entire length using a microCT system (μ CT100 Scanco Medical, Bassersdorf, Switzerland). Scan settings were: voxel size 12 μ m, medium resolution, 70 kVp, 114 μ A, 0.5 mm AL filter, and integration time 500 ms. Bone mineral density (BMD), tissue mineral density (TMD) and bone volume fraction (BV) in ossicles and vossicles were evaluated using the manufacturer's software with a fixed global threshold of 18% (180 on a grayscale of 0–1000) to segment bone from non-bone.

For intact tibiae, whole bone parameters were measured over the entire length of the bone using a 28% threshold. Tibial trabecular bone parameters were measured over a 240 μ m-long region using a threshold of 28% at a point 360 μ m distal to the growth plate. Cortical bone was measured over a 360 μ m-long region at 60% of the bone length distal to the tibio-fibular joint (TFJ) using a 28% threshold.

Histology

Upon harvest, bones, ossicles, and vossicles were fixed in 10% formalin at 4°C, and stored in 70% ethanol at room temperature until further processing. Specimens were decalcified in 10% EDTA (pH = 7.4) for 10 days, embedded in paraffin, sectioned (5 μ m), and stained with hematoxylin and eosin. Sections were imaged under brightfield, and color balance enhanced using Photoshop CS5 (ver. 12.0, Adobe Systems Inc., San Jose, CA). Total eosin-positive bone area was quantified using the thresholding function of the NIS Elements BR Software (ver. 4.12, Nikon Instruments Inc., Melville, NY).

Statistical analysis

Statistical analyses were performed using Student's t-test against the control group using SPSS Statistics software (IBM SPSS Statistics ver. 20.0, IBM Corp., Armonk NY), and a significance level $\alpha = 0.05$. Experiments were performed at least twice, with sample size noted for each experiment. Data are presented as mean \pm SEM of indicated numbers of specimens.

Results

Exogenous calcium administration regulates osteoblast number *in vitro* and *in vivo*

Calvarial osteoblastic cells isolated from neonatal wild-type mice were treated with 0–5 mM calcium chloride to determine the effect of calcium availability on cell proliferation. The number of viable cells was dependent on calcium dose, peaking with 3.5 mM CaCl_2 (Figure 1A; $p < 0.05$ vs. 0 mM CaCl_2 at each time point). A further increase in calcium did not elicit a greater increase in cell number over time.

Calcium-dependency of osteoblastic cell growth was further demonstrated *in vivo* using an ectopic BMSC ossicle model (Figure 1B). BMSC numbers were monitored *in vivo* using bioluminescent imaging (BLI) of luciferase-tagged BMSCs in scaffolds containing 0–1.2 mg calcium (Figure 1C). Similar to the *in vitro* studies, increased cell numbers were observed *in vivo* in ossicles with calcium scaffolds versus without calcium (Table 1). Ossicles containing

0.6 mg Ca²⁺ scaffolds had the greatest overall bioluminescence, reflecting cell number that peaked in week 3. A further increase in calcium did not enhance the signal.

MicroCT performed *ex vivo* after 28 days of implantation (Figure 1D) showed a significant increase in bone volume in 0.6 mg Ca²⁺ scaffolds versus calcium-free scaffolds (Figure 1E; $p = 0.03$ vs. 0 mg Ca²⁺). Histological analysis indicated a trend in bone area similar to the findings from microCT, where bone area peaked in the 0.6 mg Ca²⁺ scaffold (Supplementary Figure 1).

Calcium supports PTH effects on osteoblast proliferation and bone formation

To determine PTH and calcium interactions on bone, luciferase-labeled BMSCs seeded on scaffolds containing 0 or 0.6 mg calcium phosphate were implanted in athymic mice that were then subjected to daily PTH administration. The 0.6 mg Ca²⁺ scaffold was selected based on its robustness in the BLI and microCT findings from the dose response study. *In vivo* BLI imaging of the implants demonstrated synergistic effects of PTH and calcium on cell number (Figure 2A, B). Calcium-containing scaffold implants in animals treated with PTH had a 5.7-fold increase in BLI over scaffold implants in vehicle-treated mice ($p=0.006$, $n=8$), and a 2.4-fold increase over calcium-free scaffold implants in PTH-treated mice ($p=0.03$, $n=8$). MicroCT analysis of scaffolds after harvest (day 40) showed no effect of PTH treatment on bone volume in calcium-containing scaffold implants, but a 1.6-fold increase in bone volume in calcium-free scaffolds by daily PTH injections (Figure 2C, D; $p=0.003$, 0 mg Ca²⁺-PTH vs. vehicle, $n=8$). The number of cells per bone volume, determined as the ratio of BLI luminescence over microCT bone volume (Figure 2E), increased two-fold in calcium scaffolds with PTH treatment ($p=0.04$, PTH vs. vehicle) and 1.6-fold in scaffolds without calcium ($p=0.07$, PTH vs. vehicle). Similar trends were observed in the histologic analysis of bone area using H&E staining, where while bone area was increased 1.9-fold in calcium-free scaffold implants with PTH treatment (Figure 2F; $p=0.05$), the number of cells per bone area (BLI/bone area) was significantly increased in calcium-containing scaffold implants with PTH treatment (Figure 2G, H; $p=0.02$).

CaSR supports osteoblast survival *in vitro*

The calcium sensing receptor is a key mediator of PTH and calcium homeostasis. To determine the role of the CaSR on cell growth, calvarial cells from Col-BoneCaSR^{flox/flox} (KO) mice and control littermates (WT) were cultured and quantified *in vitro* (Figure 3A). There was no difference between the number of WT versus KO calvarial cells during initial stages of proliferation; however, after confluence (day 8), the number of WT cells continued to increase whereas KO cells reached a plateau (35% increase in WT vs. KO; $p=0.005$, $n = 7-11$).

To validate the specificity of the calcium response, a pharmacologic approach was utilized. When treated with the calcimimetic drug R-568 *in vitro*, wild-type calvarial cell numbers were unaltered from vehicle-treated cells (Figure 3B). However, treatment with the calcilytic drug NPS 2143 caused a significant decrease in cell number after confluence (32% decrease relative to vehicle; $p=0.02$, $n=4$), similar to the effect observed with the Col-BoneCaSR^{flox/flox} KO cells. To further evaluate the role of the CaSR on osteoblast

number, cell death was quantified *in vitro* (Figure 3C). Confluent cells harvested from wild-type C57/B6 mice and treated with the calcilytic had a 1.7-fold increase in cell death relative to vehicle control ($p=0.03$, $n=4$), while the calcimimetic tended to suppress cell death (72% reduction relative to vehicle, $p=0.06$).

Bone-CaSR does not affect normal bone accrual

Veterbral bodies (vossicles) isolated from $Col\text{-}BoneCaSR^{flox/flox}$ KO and control (WT) neonates were implanted in athymic mice to determine the role of the CaSR on bone accrual *in vivo* in an organ-specific manner. There was no difference in either the microCT or histological analyses of bone between the WT and KO CaSR vossicles after four weeks of implantation (Supplementary Figure 2), suggesting that the bone-specific CaSR may not be necessary for bone formation *in vivo*.

Histological analysis of H&E stained femurs from 4 days old CaSR WT and KO mice revealed no difference in bone fraction between WT and KO mice (Supplementary Figure 3B, C). MicroCT revealed no differences in bone volume or bone tissue mineral density (Supplementary Figure 3D–F; $n=6$). Gene expression of early osteoblast markers (RUNX-2, osterix, osteocalcin) measured using real-time PCR was did not differ between the two genotypes (Supplementary Figure 3G–I).

Anabolic effect of PTH is blunted in CaSR-deficient mice

PTH is anabolic in bone, yet a regulatory role of the CaSR on PTH action remains unclear. Control and KO mice received daily injections of PTH (50 $\mu\text{g}/\text{kg}$) or vehicle starting at 4 days of age for 17 days. $Col\text{-}BoneCaSR^{flox/flox}$ KO mice were significantly smaller than their control littermates (Figure 4A, B; $p=0.01$, $n=8-9$), regardless of PTH administration. Serum P1NP levels were lower in vehicle-treated $Col\text{-}BoneCaSR^{flox/flox}$ KO versus control mice (Figure 4C; $p=0.02$). PTH increased P1NP levels in control mice ($p=0.04$ vs. vehicle treatment), as well as in KO mice ($p=0.075$ vs. vehicle), hence rescuing the effect of the $Col\text{-}BoneCaSR^{flox/flox}$ KO on this bone formation marker relative to control vehicle levels. Qualitative radiographic analysis of tibiae at sacrifice suggests an increase in radiopacity in control mice and, to a lesser degree, in KO mice with PTH treatment (Figure 4D).

Histomorphometric analysis of tibiae revealed similar levels of trabecular bone volume in vehicle-treated control versus $Col\text{-}BoneCaSR^{flox/flox}$ KO mice (Figure 4E, F), both of which were markedly increased with PTH treatment when compared to corresponding vehicle-treated controls ($p<0.01$).

MicroCT analysis of tibiae showed a significantly lower BV/TV and BMD over the whole bone in $Col\text{-}BoneCaSR^{flox/flox}$ KO versus WT mice. An anabolic PTH effect was seen on BV/TV in wildtype mice, but not in $Col\text{-}BoneCaSR^{flox/flox}$ KO mice. No baseline differences in trabecular bone parameters in tibiae were found between vehicle-treated control and KO mice (Figure 5). PTH administration enhanced trabecular bone BV/TV (43%), BMD (38%), trabecular number (51%) and trabecular spacing (47%) in WT mice relative to vehicle treatment. In KO mice, PTH improved BMD and trabecular number (34% and 29% increase, respectively), and reduced trabecular spacing (33%) relative to vehicle-

treatment (all $p < 0.05$), but had no significant effect on BV/TV or trabecular thickness. Cortical bone parameters were compromised in KO mice relative to WT, and no PTH effects were observed in either genotype.

Discussion

While the complex mechanisms orchestrating the anabolic actions of PTH in bone are still under investigation, calcium availability and the calcium sensing receptor (CaSR) are potential cofactors. This study demonstrated osteoblast dependency on calcium and its synergy with PTH, and provided evidence for an adjunctive role of the CaSR in the anabolic actions of PTH.

Osteoclasts release calcium from the extracellular matrix during the process of bone resorption, thereby creating local free calcium ion concentrations of up to 40 mM [Silver et al., 1988]. Changes in calcium levels play an important role in osteoblast migration, proliferation, survival, differentiation and mineralization [Dvorak and Riccardi, 2004; Marie, 2010; Riccardi et al., 2013]. This study first demonstrated calcium dose dependency in primary calvarial osteoblastic cells *in vitro*, where cell numbers increased with calcium dose to a maximum amount and then declined. Interestingly, there was a decline in cell number in the calcium-free treatment group after switching from the initial seeding medium containing 1.8 mM CaCl_2 , suggesting the importance of calcium in retaining cell adhesion and number. Calcium dose-dependency of cell number was validated *in vivo* using an ossicle implant model [Pettway and McCauley, 2008; Pettway et al., 2008], in which cells were seeded subcutaneously in scaffolds bearing varying amounts of calcium phosphate deposits. The calcium phosphate-coated PLLA nanofiber scaffolds mimic the composition and structure of the extracellular matrix in bone, whereby the bound calcium is slowly released from the scaffold, creating a physiologically relevant environment for cell proliferation and bone formation [He et al., 2010]. BLI, microCT and histological analyses of implanted ossicles suggested a similar trend in calcium dose dependency, where 0.6 mg Ca^{2+} supported cell numbers and matrix accrual and a further increase in calcium resulted in an opposite effect. These trends suggest that $[\text{Ca}^{2+}]$ plays a dual role in regulating osteoblasts, perhaps by regulating osteoblast turnover and acting as a coupling mediator between osteoblasts and osteoclasts during bone remodeling.

Using cell implanted scaffolds containing 0 mg and 0.6 mg calcium phosphate, PTH had a greater effect on cell number *in vivo* in the presence of calcium. PTH had a greater effect on bone volume in scaffolds without calcium, but there was increase in the number of cells per bone volume with the combined calcium and PTH treatment; however, similar trends did not exist in bone volume and bone area. The increased total number of cells resulting from the combination of PTH and calcium may include differentiated BMSCs that are not specific to the osteoblastic lineage, thus accounting for the different patterns in cell number versus bone volume. The bone marrow contains a diverse population of cells, including fibroblasts, endothelial cells, reticulocytes, adipocytes and mesenchymal cells, which can be driven towards the osteoblast, adipocyte or chondrocyte lineages [Caplan, 1991]. The osteoblast lineage can be directed by treating BMSCs *in vitro* with dexamethasone [Cheng et al., 1994; Maniopoulos et al., 1988; Peter et al., 1998], as was initially performed in this study. This

treatment, while effective in increasing alkaline phosphate (ALP) activity, osteocalcin expression, bone sialoprotein expression and matrix mineralization, also promotes the adipocyte lineage [Bennett et al., 1991; Beresford et al., 1992]. In a similar ossicle model where BMSCs were seeded onto gelatin sponges and implanted ectopically in immunodeficient mice, both PTH and vehicle treatment supported adipose cell number [Pettway et al., 2005]. Therefore, the increase in cell number, demonstrated using bioluminescence, may include a population of non-osteoblastic cells, and potentially explains why an increase in cell number does not correlate with tissue level alterations.

One proposed mediator involved in calcium and PTH interactions is the CaSR. While the presence of the CaSR has been demonstrated in osteoblasts [Chattopadhyay et al., 2004; Kameda et al., 1998; Yamaguchi et al., 1998; Yamaguchi et al., 2001], its function has been largely controversial and not well understood, as osteoblasts lacking CaSR are still able to sense and respond to extracellular calcium [Fromigué et al., 2009; Pi et al., 2000], potentially through other cation-sensing receptors such as the G-protein coupled receptor, GPRC6A [Pi et al., 2005], or alternatively spliced CaSR variants missing exon 5 that continue to be expressed even with a global CaSR deletion of full-length CaSRs [Rodriguez et al., 2005]. The findings in this study suggest that the CaSR, in fact, plays a critical protective role in osteoblast survival.

Absence of the CaSR had no effect on the number of osteoblastic cells during early stages in culture. However, after confluence (approx. day 8 in culture), wild-type cells continued to increase in number whereas osteoblast-specific CaSR knock-out cells plateaued. Treatment of wild-type cells with a calcilytic agent significantly reduced the number of cells at confluence relative to vehicle and calcimimetic treatment. While the osteoblast-specific CaSR knock-out had a similar effect as the calcilytic treatment, the latter had a greater impact on cell number likely because the calcilytic agent acts as agonist to the CaSR in all cell types. CaSR gene expression has been shown to increase in mature osteoblasts during later stages in culture [Chattopadhyay et al., 2004], supporting the above findings.

Quantitative real-time PCR indicated similar expression levels of important early osteoblast markers RUNX-2, osterix and osteocalcin between CaSR knock-out and wild-type mice. These results are in contrast with earlier findings showing a decrease in osteoblast gene expression markers [Chang et al., 2008], and may reflect intrinsic differences between the calvarial osteoblasts in the present study and bone marrow-derived osteoblasts. Interestingly, while the CaSR knock-out phenotype has reduced bone quality in adult mice [Brown et al., 1998; Chang et al., 2008; Garner et al., 2001; Ho et al., 1995; Riccardi et al., 2013; Tu et al., 2003], microCT and histologic analyses of neonatal CaSR control and knock-out mice showed no differences in bone parameters of young mice. Together, these findings suggest that the role of the CaSR is less pronounced in young mice, and supports the *in vitro* findings proposing the importance of the CaSR in mature osteoblasts and cell survival.

In the present study, vertebral bodies from young CaSR control and Col-BoneCaSR^{flx/flx} osteoblast-specific knock-out mice had comparable levels of trabecular bone four weeks after implantation. The CaSR knock-out also did not have an effect on trabecular bone parameters of vehicle-treated intact mice. Together, these findings indicate that trabecular

bone formation can occur independently of the osteoblast-specific CaSR and may be supplemented by normal endocrine signaling from the host mouse. The robust PTH effect on wild-type mice was seen to a lesser extent in osteoblast-specific CaSR knock-out mice, with an improvement in serum PINP levels but no net significant effect on trabecular bone volume, suggesting that the anabolic actions of PTH are at least partially dependent on the CaSR.

Cortical bone microCT parameters, however, were compromised in the osteoblast-specific CaSR knock-out, suggesting a more significant role for the CaSR in cortical bone. Whole bone parameters were reduced and PTH effects were abolished by the osteoblast-specific CaSR knock-out. These findings are consistent with a proposed compartmental role for the CaSR on PTH effects in bone, where the CaSR is thought to have a larger effect on cortical bone than trabecular bone [Xue et al., 2012], and suggest a role for the CaSR in the anabolic effects of PTH.

In summary, osteoblast numbers *in vitro* and bone volume *in vivo* depend on calcium suggesting that the CaSR is important for osteoblast activity. Trabeculation occurred normally in osteoblast-specific CaSR knock-out mice and vertebral implants, suggesting that the CaSR is dispensable for trabecular bone formation. However, whole and cortical bone parameters were significantly compromised by the loss of the osteoblast-specific CaSR, and PTH effects were abolished in these mice. These findings suggest that the CaSR is part of an endocrine signaling pathway that plays an important role in the anabolic actions of PTH.

Supplementary Material

Refer to Web version on PubMed Central for supplementary material.

Acknowledgments

This work was supported by funding from the NIH grant DE022327-02 and AR067291, and DOD grant W81XWH-12-2-0008. The authors would like to thank the Department of Radiology at The University of Michigan for the use of The Center for Molecular Imaging, which is supported in part by NIH grant P50 CA093990, as well as Christa Guest for her assistance in genotyping CaSR litters, Stephanie Daignault-Newton for statistical consultation, and Paul Kostenuik and Melanie Gupte for critical reading of the manuscript.

References

- Bashutski JD, Eber RM, Kinney JS, Benavides E, Maitra S, Braun TM, Giannobile WV, McCauley LK. Teriparatide and osseous regeneration in the oral cavity. *New England Journal of Medicine*. 2010; 363:2396–405. [PubMed: 20950166]
- Bennett JH, Joyner CJ, Triffitt JT, Owen ME. Adipocytic cells cultured from marrow have osteogenic potential. *Journal of Cell Science*. 1991; 99(Pt 1):131–9. [PubMed: 1757497]
- Beresford JN, Bennett JH, Devlin C, Leboy PS, Owen ME. Evidence for an inverse relationship between the differentiation of adipocytic and osteogenic cells in rat marrow stromal cell cultures. *Journal of Cell Science*. 1992; 102(Pt 2):341–51. [PubMed: 1400636]
- Boden SD, Kaplan FS. Calcium homeostasis. *Orthopedic Clinics of North America*. 1990; 21:31–42. [PubMed: 2404236]
- Brown EM. The calcium-sensing receptor: physiology, pathophysiology and CaR-based therapeutics. *Subcellular Biochemistry*. 2007; 45:139–67. [PubMed: 18193637]
- Brown EM, MacLeod RJ. Extracellular calcium sensing and extracellular calcium signaling. *Physiological Reviews*. 2001; 81:239–297. [PubMed: 11152759]

- Brown EM, Pollak M, Hebert SC. The extracellular calcium-sensing receptor: its role in health and disease. *Annual Review of Medicine*. 1998; 49:15–29.
- Caplan AI. Mesenchymal stem cells. *Journal of Orthopedic Research*. 1991; 9:641–50.
- Chang W, Tu C, Chen TH, Bikle D, Shoback D. The extracellular calcium-sensing receptor (CaSR) is a critical modulator of skeletal development. *Science Signaling*. 2008; 1:ra1. [PubMed: 18765830]
- Chattopadhyay N, Yano S, Tfelt-Hansen J, Rooney P, Kanuparthi D, Bandyopadhyay S, Ren X, Terwilliger E, Brown EM. Mitogenic action of calcium-sensing receptor on rat calvarial osteoblasts. *Endocrinology*. 2004; 145:3451–62. [PubMed: 15084499]
- Chen H-L, Demiralp B, Schneider A, Koh AJ, Silve C, Wang C-Y, McCauley LK. Parathyroid hormone and parathyroid hormone-related protein exert both pro- and anti-apoptotic effects in mesenchymal cells. *Journal of Biological Chemistry*. 2002; 277:19374–19381. [PubMed: 11897779]
- Cheng SL, Yang JW, Rifas L, Zhang SF, Avioli LV. Differentiation of human bone marrow osteogenic stromal cells in vitro: induction of the osteoblast phenotype by dexamethasone. *Endocrinology*. 1994; 134:277–86. [PubMed: 8275945]
- Cheng Z, Liang N, Chen TH, Li A, Santa Maria C, You M, Ho H, Song F, Bikle D, Tu C, Shoback D, Chang W. Sex and age modify biochemical and skeletal manifestations of chronic hyperparathyroidism by altering target organ responses to Ca²⁺ and parathyroid hormone in mice. *Journal of Bone and Mineral Research*. 2013; 28:1087–100. [PubMed: 23239173]
- Dvorak MM, Riccardi D. Ca²⁺ as an extracellular signal in bone. *Cell Calcium*. 2004; 35:249–55. [PubMed: 15200148]
- Fromig   O, Ha   E, Barbara A, Petrel C, Traiffort E, Ruat M, Marie PJ. Calcium sensing receptor-dependent and receptor-independent activation of osteoblast replication and survival by strontium ranelate. *Journal of cellular and molecular medicine*. 2009; 13:2189–2199. [PubMed: 20141614]
- Garner SC, Pi M, Tu Q, Quarles LD. Rickets in cation-sensing receptor-deficient mice: an unexpected skeletal phenotype. *Endocrinology*. 2001; 142:3996–4005. [PubMed: 11517179]
- Goltzman D, HENDY GN. The calcium-sensing receptor in bone--mechanistic and therapeutic insights. *Nature Reviews Endocrinology*. 2015; 11:298–307.
- He C, Xiao G, Jin X, Sun C, Ma PX. Electrodeposition on nanofibrous polymer scaffolds: Rapid mineralization, tunable calcium phosphate composition and topography. *Advanced Functional Materials*. 2010; 20:3568–3576. [PubMed: 21673827]
- Ho C, Conner DA, Pollak MR, Ladd DJ, Kifor O, Warren HB, Brown EM, Seidman JG, Seidman CE. A mouse model of human familial hypocalciuric hypercalcemia and neonatal severe hyperparathyroidism. *Nature Genetics*. 1995; 11:389–94. [PubMed: 7493018]
- Kameda T, Mano H, Yamada Y, Takai H, Amizuka N, Kobori M, Izumi N, Kawashima H, Ozawa H, Ikeda K, Kameda A, Hakeda Y, Kumegawa M. Calcium-sensing receptor in mature osteoclasts, which are bone resorbing cells. *Biochemical and Biophysical Research Communications*. 1998; 245:419–422. [PubMed: 9571166]
- Koh AJ, Demiralp B, Neiva KG, Hooten J, Nohutcu RM, Shim H, Datta NS, Taichman RS, McCauley LK. Cells of the osteoclast lineage as mediators of the anabolic actions of parathyroid hormone in bone. *Endocrinology*. 2005; 146:4584–96. [PubMed: 16081645]
- Koh AJ, Novince CM, Li X, Wang T, Taichman RS, McCauley LK. An irradiation-altered bone marrow microenvironment impacts anabolic actions of PTH. *Endocrinology*. 2011; 152:4525–4536. [PubMed: 22045660]
- Kos CH, Karaplis AC, Peng J-B, Hediger MA, Goltzman D, Mohammad KS, Guise TA, Pollak MR. The calcium-sensing receptor is required for normal calcium homeostasis independent of parathyroid hormone. *The Journal of Clinical Investigation*. 2003; 111:1021–1028. [PubMed: 12671051]
- Kostenuik PJ, Smith SY, Samadfam R, Jollette J, Zhou L, Ominsky MS. Effects of denosumab, alendronate, or denosumab following alendronate on bone turnover, calcium homeostasis, bone mass and bone strength in ovariectomized cynomolgus monkeys. *Journal of Bone and Mineral Research*. 2015; 30:657–69. [PubMed: 25369992]
- Liao J, Schneider A, Datta NS, McCauley LK. Extracellular calcium as a candidate mediator of prostate cancer skeletal metastasis. *Cancer Research*. 2006; 66:9065–73. [PubMed: 16982748]

- Lieben L, Masuyama R, Torrekens S, Van Looveren R, Schrooten J, Baatsen P, Lafage-Proust MH, Dresselaers T, Feng JQ, Bonewald LF, Meyer MB, Pike JW, Bouillon R, Carmeliet G. Normocalcemia is maintained in mice under conditions of calcium malabsorption by vitamin D-induced inhibition of bone mineralization. *Journal of Clinical Investigation*. 2012; 122:1803–15. [PubMed: 22523068]
- Maniopoulos C, Sodek J, Melcher AH. Bone formation in vitro by stromal cells obtained from bone marrow of young adult rats. *Cell and Tissue Research*. 1988; 254:317–30. [PubMed: 3197089]
- Marie PJ. The calcium-sensing receptor in bone cells: a potential therapeutic target in osteoporosis. *Bone*. 2010; 46:571–576. [PubMed: 19660583]
- Miyauchi A, Hruska KA, Greenfield EM, Duncan R, Alvarez J, Barattolo R, Colucci S, Zamboni-Zallone A, Teitelbaum SL, Teti A. Osteoclast cytosolic calcium, regulated by voltage-gated calcium channels and extracellular calcium, controls podosome assembly and bone resorption. *The Journal of Cell Biology*. 1990; 111:2543–2552. [PubMed: 1703539]
- Mundy GR, Guise TA. Hormonal control of calcium homeostasis. *Clinical Chemistry*. 1999; 45:1347–52. [PubMed: 10430817]
- Ota K, Quint P, Ruan M, Pederson L, Westendorf JJ, Khosla S, Oursler MJ. TGF-beta induces Wnt10b in osteoclasts from female mice to enhance coupling to osteoblasts. *Endocrinology*. 2013; 154:3745–52. [PubMed: 23861379]
- Peter SJ, Liang CR, Kim DJ, Widmer MS, Mikos AG. Osteoblastic phenotype of rat marrow stromal cells cultured in the presence of dexamethasone, beta-glycerolphosphate, and L-ascorbic acid. *Journal of Cellular Biochemistry*. 1998; 71:55–62. [PubMed: 9736454]
- Pettway GJ, McCauley LK. Ossicle and vossicle implant model systems. *Methods in Molecular Biology*. 2008; 455:101–10. [PubMed: 18463813]
- Pettway GJ, Meganck JA, Koh AJ, Keller ET, Goldstein SA, McCauley LK. Parathyroid hormone mediates bone growth through the regulation of osteoblast proliferation and differentiation. *Bone*. 2008; 42:806–18. [PubMed: 18234576]
- Pettway GJ, Schneider A, Koh AJ, Widjaja E, Morris MD, Meganck JA, Goldstein SA, McCauley LK. Anabolic actions of PTH (1–34): use of a novel tissue engineering model to investigate temporal effects on bone. *Bone*. 2005; 36:959–70. [PubMed: 15878317]
- Pi M, Faber P, Ekema G, Jackson PD, Ting A, Wang N, Fontilla-Poole M, Mays RW, Brunden KR, Harrington JJ, Quarles LD. Identification of a novel extracellular cation-sensing G-protein-coupled receptor. *Journal of Biological Chemistry*. 2005; 280:40201–40209. [PubMed: 16199532]
- Pi M, Garner SC, Flannery P, Spurney RF, Quarles LD. Sensing of extracellular cations in CasR-deficient osteoblasts. Evidence for a novel cation-sensing mechanism. *Journal of Biological Chemistry*. 2000; 275:3256–3263. [PubMed: 10652312]
- Poole KE, Reeve J. Parathyroid hormone - a bone anabolic and catabolic agent. *Current Opinions in Pharmacology*. 2005; 5:612–7.
- Riccardi D, Brennan SC, Chang W. The extracellular calcium-sensing receptor, CaSR, in fetal development. *Journal of Clinical Endocrinology and Metabolism*. 2013; 27:443–453.
- Rodriguez L, Tu C, Cheng Z, Chen TH, Bikle D, Shoback D, Chang W. Expression and functional assessment of an alternatively spliced extracellular Ca²⁺-sensing receptor in growth plate chondrocytes. *Endocrinology*. 2005; 146:5294–303. [PubMed: 16166224]
- Silver IA, Murrills RJ, Etherington DJ. Microelectrode studies on the acid microenvironment beneath adherent macrophages and osteoclasts. *Experimental Cell Research*. 1988; 175:266–276. [PubMed: 3360056]
- Sugimoto T, Kanatani M, Kano J, Kaji H, Tsukamoto T, Yamaguchi T, Fukase M, Chihara K. Effects of high calcium concentration on the functions and interactions of osteoblastic cells and monocytes and on the formation of osteoclast-like cells. *Journal of Bone and Mineral Research*. 1993; 8:1445–1452. [PubMed: 8304045]
- Tang Y, Wu X, Lei W, Pang L, Wan C, Shi Z, Zhao L, Nagy TR, Peng X, Hu J, Feng X, Van Hul W, Wan M, Cao X. TGF-beta1-induced migration of bone mesenchymal stem cells couples bone resorption with formation. *Nature Medicine*. 2009; 15:757–65.

- Tu Q, Pi M, Karsenty G, Simpson L, Liu S, Quarles LD. Rescue of the skeletal phenotype in CasR-deficient mice by transfer onto the Gcm2 null background. *Journal of Clinical Investigation*. 2003; 111:1029–1037. [PubMed: 12671052]
- Wei G, Ma PX. Macroporous and nanofibrous polymer scaffolds and polymer/bone-like apatite composite scaffolds generated by sugar spheres. *Journal of Biomedical Materials Research Part A*. 2006; 78:306–315. [PubMed: 16637043]
- Wu X, Pang L, Lei W, Lu W, Li J, Li Z, Frassica FJ, Chen X, Wan M, Cao X. Inhibition of Sca-1-positive skeletal stem cell recruitment by alendronate blunts the anabolic effects of parathyroid hormone on bone remodeling. *Cell Stem Cell*. 2010; 7:571–80. [PubMed: 21040899]
- Xue Y, Xiao Y, Liu J, Karaplis AC, Pollak MR, Brown EM, Miao D, Goltzman D. The calcium-sensing receptor complements parathyroid hormone-induced bone turnover in discrete skeletal compartments in mice. *American Journal of Physiology: Endocrinology Metabolism*. 2012; 302:E841–51. [PubMed: 22275754]
- Yamaguchi T, Chattopadhyay N, Kifor O, Butters RR Jr, Sugimoto T, Brown EM. Mouse osteoblastic cell line (MC3T3-E1) expresses extracellular calcium (Ca²⁺)-sensing receptor and its agonists stimulate chemotaxis and proliferation of MC3T3-E1 cells. *Journal of Bone and Mineral Research*. 1998; 13:1530–1538. [PubMed: 9783541]
- Yamaguchi T, Chattopadhyay N, Kifor O, Ye C, Vassilev PM, Sanders JL, Brown EM. Expression of extracellular calcium-sensing receptor in human osteoblastic MG-63 cell line. *American Journal of Physiology: Cell Physiology*. 2001; 280:C382–393. [PubMed: 11208534]
- Zaidi M, Datta HK, Patchell A, Moonga B, MacIntyre I. 'Calcium-activated' intracellular calcium elevation: a novel mechanism of osteoclast regulation. *Biochemical and Biophysical Research Communications*. 1989; 163:1461–1465. [PubMed: 2783143]

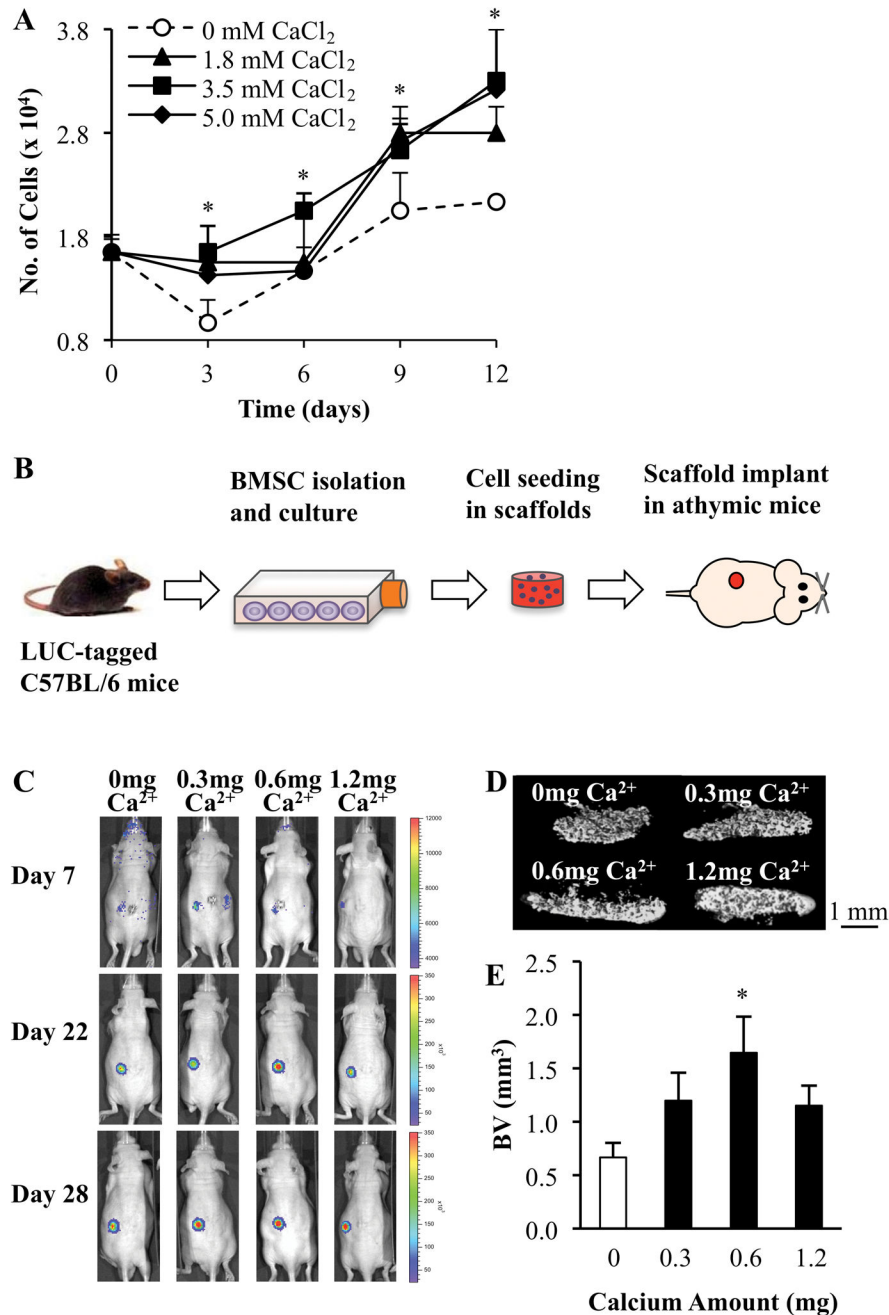


Fig. 1. Osteoblasts and bone volume are influenced by calcium availability

(A) Calvarial osteoblast numbers are dependent on exogenous calcium concentration *in vitro*. Cell number increased dose-dependently and reached a maximum with 3.5 mM CaCl₂ treatment (* p<0.05 relative to no calcium, n=4/gp). (B) Schematic illustration of ossicle experiment. BMSCs were isolated from long bones of luciferase-tagged C57BL/6 mice, expanded *in vitro* and seeded (1×10⁶ cells/ossicle) in PLLA-based scaffolds. Scaffolds were implanted in athymic mice and left for 28 days, with regular *in vivo* monitoring using bioluminescence (BLI). (C) BLI imaging was used to monitor cell number post-implantation. Representative microCT images (D) and analysis (E) of scaffolds after harvest

indicated a significant increase in bone volume in the 0.6 mg Ca²⁺ scaffold. (Data is mean ± SEM, n=8/gp; * p<0.05 relative to 0 mg Ca²⁺).

Author Manuscript

Author Manuscript

Author Manuscript

Author Manuscript

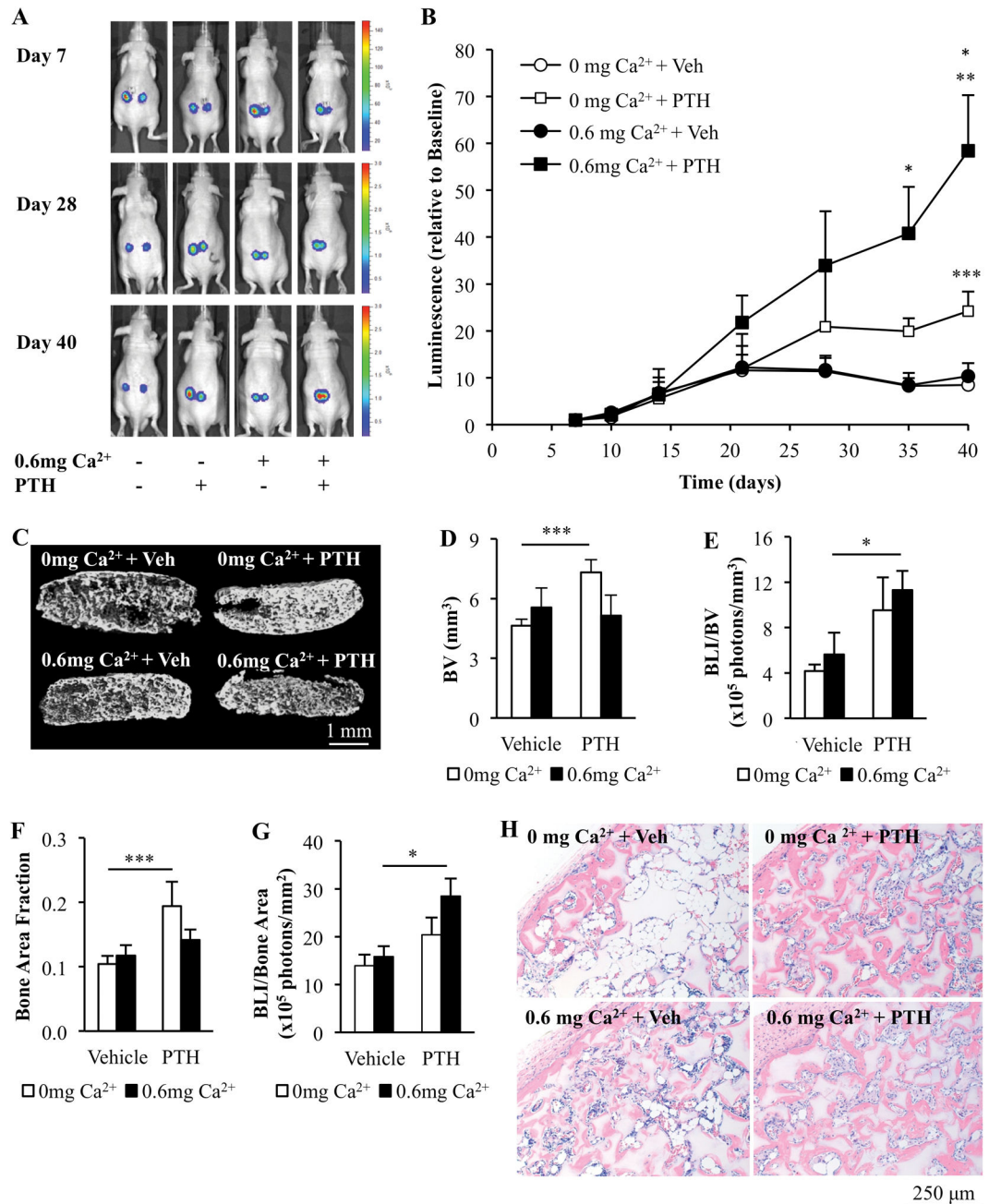


Fig. 2. Calcium enhanced PTH effects on osteoblast number *in vivo*

(A) Representative BLI images of mice implanted with scaffolds (0 mg vs. 0.6 mg Ca²⁺) seeded with luciferase-tagged BMSCs. (B) PTH administration significantly increased luminescence reflecting increased cell number relative to vehicle which was further enhanced by calcium (0.6 mg Ca²⁺) relative to calcium-free (0 mg Ca²⁺) scaffolds. Representative images (C) and analysis (D) of scaffolds on day 40 using microCT suggested a PTH effect in scaffolds with no calcium. (E) BLI/BV, reflecting the number of cells per bone volume, was significantly increased by the combination of calcium and PTH. (F) Histological analysis of osseous matrix area relative to total scaffold area using H&E

staining revealed an increase in mineralized tissue in Ca-free scaffolds with PTH treatment but not in calcium scaffolds. (G) There was no difference in cell number (BLI) per bone area (histology) between calcium and calcium-free scaffolds within treatment groups, but a significant increase was found in calcium scaffolds with PTH. (H) Representative images of scaffolds. Unstained (grey/white) areas indicate remaining scaffold particles, whereas pink denotes eosin-positive bone matrix. (Data is mean \pm SEM, n = 8/gp; * p<0.05 PTH + 0.6 mg Ca²⁺ vs. Veh + 0.6 mg Ca²⁺, ** p<0.05 PTH + 0.6 mg Ca²⁺ vs. PTH + 0 mg Ca²⁺, *** p<0.05 PTH + 0 mg Ca²⁺ vs. Veh + 0 mg Ca²⁺).

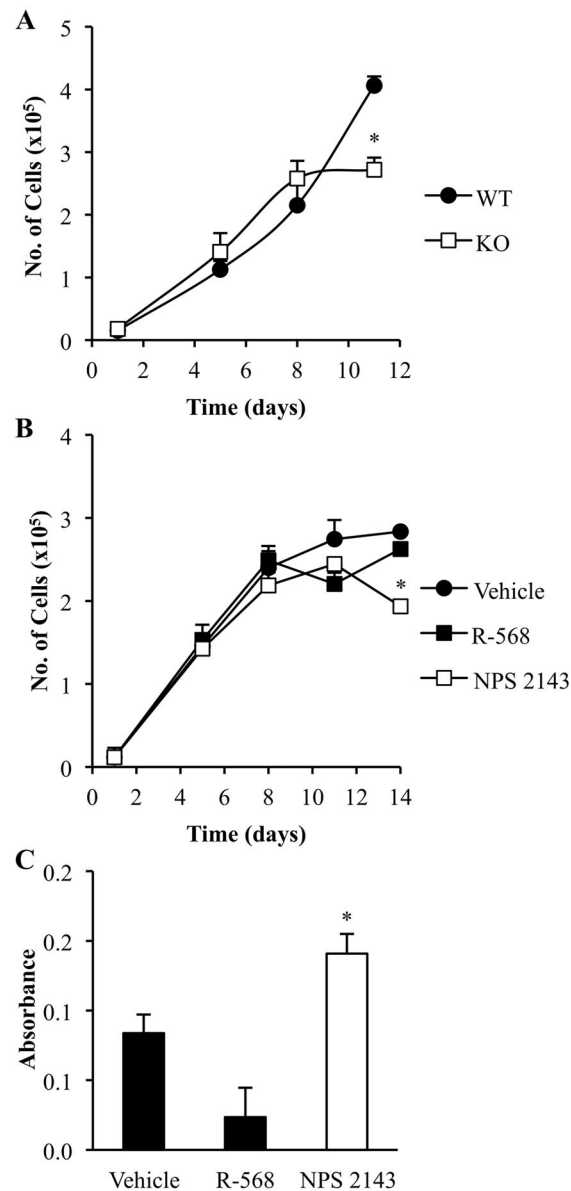


Fig. 3. Presence of the CaSR supports osteoblast survival *in vitro*

Calvarial cell culture from osteoblast-specific CaSR knock-out mice ($Col-BoneCaSR^{flox/flox}$; KO) and control littermates (WT). (A) There were no differences between the number of KO and WT calvarial osteoblasts during the initial days of culture. However, after cells reached confluence the number of WT cells continued to increase, whereas KO cells plateaued. ($n=7-11/gp$, $*p<0.05$ KO relative to WT cells). (B) Pharmacologic treatment of WT cells with a CaSR agonist (calcimimetic, R-568) or antagonist (calcilytic, NPS 2143) had no effect on cell number during the initial days of culture, but NPS 2143 caused cell number to decline after cells reached confluence. (C) Measurement of DNA fragmentation revealed an increase in apoptosis with NPS 2143 treatment on day 14 relative to the other treatment groups. ($n=4/gp$ for B-C, $*p<0.05$ relative to both vehicle and calcimimetic treatment). All data is mean \pm SEM.

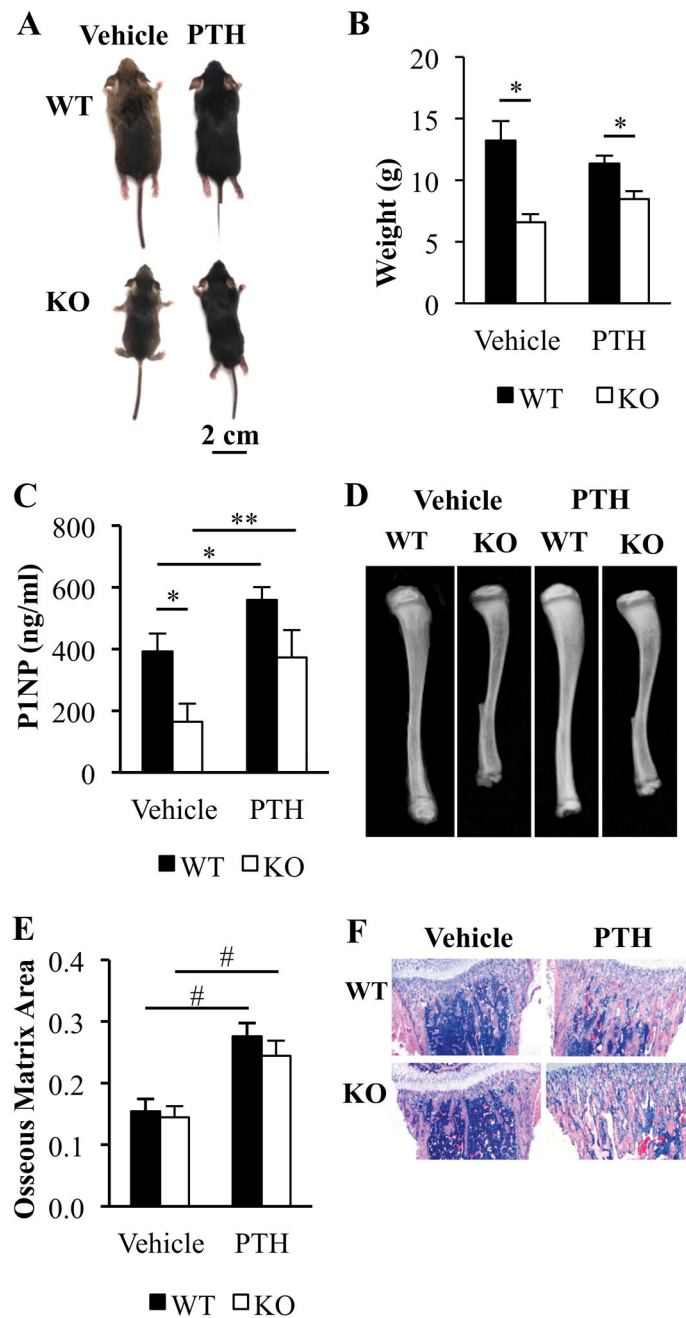


Fig. 4. PTH effects on body weight, serum P1NP and tibial radiography in WT vs. Col-BoneCaSR flox/flox mice

(A) Images of 21-day-old WT and KO littermates after 17 days of vehicle or PTH treatment. (B) Mouse total body weight was significantly lower in KO mice, with no PTH effect in either WT or KO mice. (C) Serum P1NP levels were significantly reduced in KO vs. WT vehicle-treated mice. PTH treatment increased P1NP levels in WT mice, and normalized the effect of the Col-BoneCaSR flox/flox KO to WT-vehicle levels. (n=8–9 for B–C; * p<0.05 relative to WT control in each treatment group.) (D) KO tibiae appeared smaller and more radiolucent than WT. PTH treatment increased radiopacity of both KO and WT bones. (E)

Histologic analysis revealed that osseous bone matrix area was not affected by the Col1-CaSR KO, and was increased with PTH treatment in both WT and KO mice (n=8–9/gp; # p<0.01 relative to vehicle treatment). (F) Representative images of H&E staining of mouse tibiae. All data are mean \pm SEM.

Author Manuscript

Author Manuscript

Author Manuscript

Author Manuscript

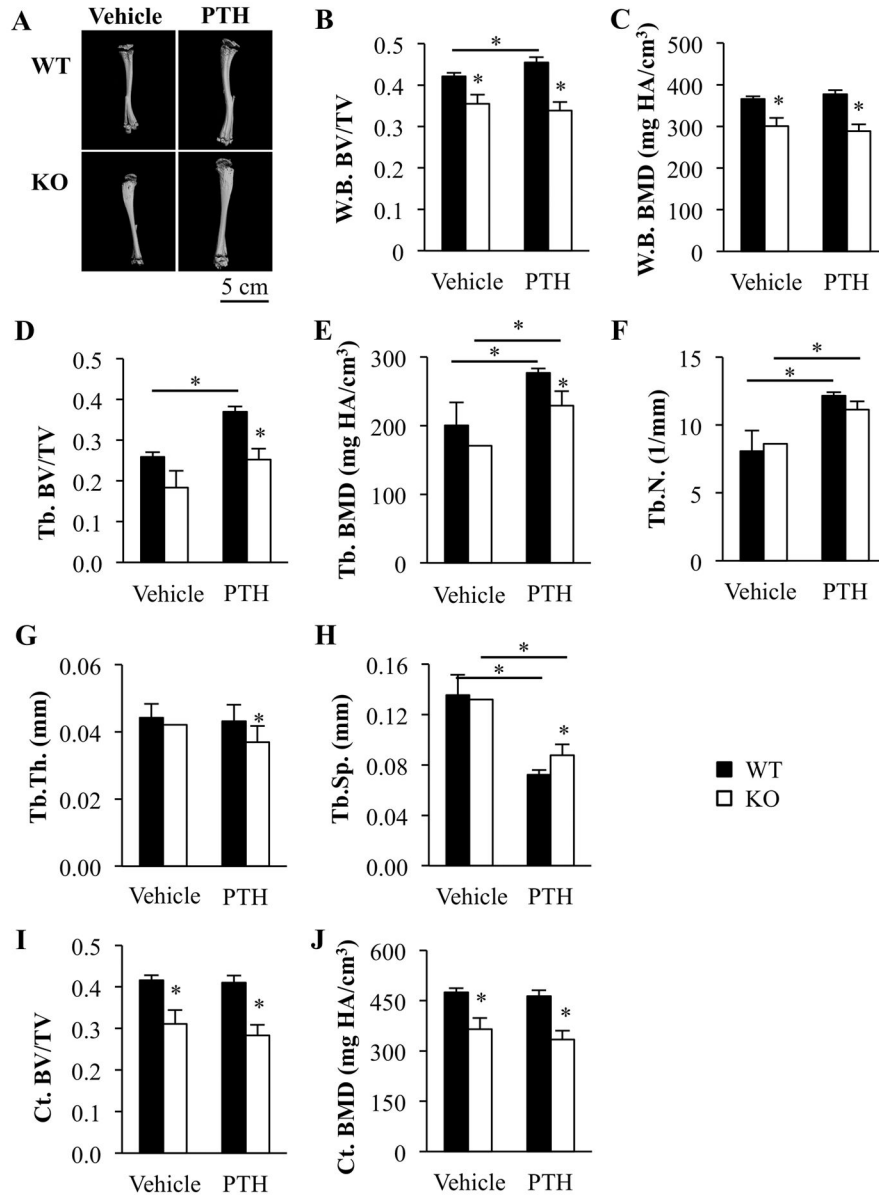


Fig. 5. PTH effects on microCT parameters in WT vs. Col1-CaSR KO mice

MicroCT reconstruction (A) and analysis (B–J) of Col1-CaSR WT and KO tibiae revealed significant differences between WT and KO mice in both vehicle and PTH-treated mice. (B–C) The anabolic actions of PTH on whole tibiae (W.B. – whole bone) were diminished in Col1-CaSR KO mice. (D–H) No differences in trabecular bone (Tb.) parameters (BV/TV, BMD, Tb.N. – trabecular number, Tb.Th. trabecular thickness, Tb.Sp. – trabecular spacing) between vehicle-treated WT and KO mice. A consistent PTH effect was seen in trabecular bone parameters of WT mice, and to a lesser extent in the KO mice but not in trabecular BV/TV of KO mice. (I–J) Cortical bone (Ct.) parameters (BV/TV, BMD) were significantly compromised in Col1-CaSR KO mice, and PTH did not alter cortical parameters in either

group. (Data are mean \pm SEM, n = 8/gp; * p<0.05 relative to WT control in the same treatment group, unless otherwise indicated).

Author Manuscript

Author Manuscript

Author Manuscript

Author Manuscript

Table 1

Bioluminescence (BLI) measurements in scaffolds from two experiments

Scaffold	Experiment 1 (n = 4/gp)				Experiment 2 (n = 8/gp)			
	Week 1	Week 2	Week 3	Week 4	Week 1	Week 2	Week 3	Week 4
0 mg Ca ²⁺	1.6 ± 0.1	3.0 ± 0.2	4.3 ± 0.3	2.4 ± 0.4	2.7 ± 0.4	7.7 ± 1.6	65 ± 26	85 ± 30
0.3 mg Ca ²⁺	3.5 ± 0.2	10 ± 1.4	8.7 ± 0.5	7.0 ± 0.1	2.8 ± 0.3	17 ± 3.7	87 ± 15	107 ± 25
0.6 mg Ca ²⁺	6.9 ± 1.5*	13 ± 0.6*	12 ± 0.6#	6.0 ± 0.3*	2.6 ± 0.6	11 ± 3.4	110 ± 19	100 ± 27
1.2 mg Ca ²⁺	5.2 ± 1.5	16 ± 1.5*	14 ± 0.8*	3.5 ± 0.9	2.8 ± 0.9	21 ± 10.7	96 ± 21	89 ± 15

NB: Experiment 1 was performed using 1×10 cells per scaffold initial seeding; experiment 2 was performed using 2.5×10⁶ cells per scaffold. No significance was observed within experiment 2, but trends were similar as experiment 1. Data is reported as photons x 10⁻⁴.

* p < 0.05 and

p = 0.06 vs. 0 mg Ca²⁺ at each time point.